A comparison of the neumann-kelvin and rankine source methods for wave resistance calculations

Min Yu* and Jeffrey Falzarano[a]

Department of Ocean Engineering, Texas A&M University, 400 Bizzell St, College Station, Texas 77840, United States

Abstract. Calm water wave resistance plays a very important role in ship hull design. Numerical methods are meaningful for this reason. In this study, two prevailing methods, the Neumann-Kelvin and the Rankine source method, were implemented and compared. The Neumann-Kelvin method assumes linearized free surface boundary condition and only needs to mesh the hull surface. The Rankine source method considers nonlinear free surface boundary condition and meshes both the ship hull surface and free surface. Both methods were implemented and the wave resistance of a Wigley III and three Series 60(Cb=0.6, 0.7, 0.8) hulls were analyzed. The results were compared with experimental results and the merits of both numerical techniques were quantified. Based on the results, it is concluded that the Rankine source method is more accurate in the calculation of the wave-making resistance. Using the Neumann-Kelvin method, it is found to be easier to model the hull and can be used for slender ships to solve problems like wave current coupling calculation.

Keywords: calm water wave resistance; Neumann-Kelvin method; rankine source method; experiment; nonlinear free surface boundary condition

1. Introduction

Calm water resistance is mainly composed of wave-making and frictional resistance. For a given ship speed, frictional resistance is in proportion to the wetted surface area. Since the wetted surface does not vary greatly for a given ship displacement, the change of frictional resistance is limited. However, for a given Froude number, wave-making resistance is extremely sensitive to the shape of the ship hull. Modification of the hull shape can significantly decrease wave-making resistance, thus the optimization of wave-making resistance is very important.

The mathematical model of wave-making resistance is not difficult, however, the solution of governing equations is not a challenging task due to the nonlinearity of the boundary conditions. First, the shape of ship hull surface is nonlinear; second, the free surface boundary condition contains nonlinear terms; third, the free surface boundary is satisfied on unknown free surface, which is usually nonlinear. Moreover, the free surface can only be obtained after solving Laplace's equation,

---

*Corresponding author, E-mail: yu3069@tamu.edu
[a]Professor, E-mail: jfalzarano@tamu.edu

which makes the process of solution iterative. Due to these difficulties, there is not a closed form analytic solution to the wave-making resistance problem.

Background on literature survey, the first stage of research in wave-resistance calculation was the linear theory, which solves the problem using linearized boundary conditions, for example, Michell's thin ship theory (Michell 1898). The linearization of the boundary conditions brings convenience in calculation, even analytical solution can be derived. However, linear ship theory is only effective under the assumption that the hull form is linear (very thin or very flat) and the free surface boundary condition is also linear(wave height is small compared to wave length). These assumptions are violated for realistic hull forms, thus the linear theory can not give satisfactory result for realistic hull forms.

Following the linear theory, the Neumann-Kelvin method appeared. The Neumann-Kelvin method satisfies an accurate hull surface boundary condition but only satisfies the linearized free surface boundary condition on the calm water surface. In the Neumann-Kelvin method, the Kelvin sources are distributed on the ship hull surface. Michell (1898), Havelock (1928, 1932) and Peters (1949) gave the analytic expressions of the velocity potential of the translating point source, which is called the Green's function. Noblesse (1981) analyzed different expressions of the Green's function and fitted them into a unified form. According to Noblesse's remarkable work, the Green's function is composed of three parts. The first part is the Rankine source part, it indicates the influence of point source in an infinite fluid domain, Hess and Smith (1962, 1967) derived the velocity potential generated by point sources distributed on a flat panel. The second part of the Green's function is the double integral part, which represents the near-field disturbance of the point source in a fluid domain with the free surface. Newman (1987) calculated the double integral part by sum of Chebyshev series and an additional term for the singularity; Ponizy and Noblesse (1994) gave the result of the double integral by numerical interpolation. The third part of the Green's function is the single integral part, which represents the far-field disturbance. The numerical calculation of the single integral part is difficult because the integrand is highly oscillatory(Baar 1986, Baar and Price 1988). One way to calculate the single integral part involves two expansions given by Bessho (1964). Ursell (1960) derived an additional term and make these two expansions completely complementary. Numerical result of this method were given by Baar (1986), Ursell (1960), Marr (1996), Wang and Rogers (1989). The other way to calculate the single integral part is by the numerical integration. However, due to the oscillatory behavior of the integrand, the typical numerical integration methods (e.g., the Simpson method or the adaptive method(Abramowitz and Stegun 1964)) are extremely inefficient. So new method must be applied in the numerical calculation of the single integral part. One such method is developed by Levin (1982, 1997). Levin's method convert the calculation of an integral into the calculation of an partial differential equation. However, when Levin's method is applied to the single integral part of the Green's function, Faddeyeva function(Faddeyeva *et al.* 1961) need to be calculated, which is difficult and time consuming. The other numerical integral method is the deepest descend method(Motygin 2014). This method convert the oscillatory integrand into a non-oscillatory one. Then the routine numerical integration methods can be used in the calculation.

As the research about wave-making resistance goes on, the nonlinear methods came into being. Maruo (1966) and Eggers (1966) developed the second order thin ship theory. In their study, the Taylor expansion was used and it caused contradictions at the ship's bow and stern. Wehausen (1967) and Yim (1968) improved the second order theory by mapping the free surface and hull surface into

a reference domain. Another variant of the second order method is Guilloton's method(Guilloton 1964, 1965). This method maps the result of linear Michell theory into a better approximation by inverse streamline tracing method. Among the nonlinear methods, the Rankine source method is a promising one. Dawson (1977) calculated wave-making resistance by this method. His method started from the result of double model flow and then calculated the disturbance of this base flow. He also applied a forward difference scheme to the free surface boundary condition to satisfy the radiation condition. Dawson's method can get accurate result for some realistic hull forms. However, there are some problems with the Rankine source method. One is the numerical dispersion due to the use of the different scheme in the free surface boundary condition(Han and Olson 1987a, Schultz and Hong 1989a). Schultz and Hong (1989a) and Cao (1991a) developed the raised panel method. In their study, the panels were at some distance over the free water surface to reduce the numerical dispersion. Another problem with the Rankine source method is the oscillation of panel source strength(Raven 1998). To solve this problem, Raven (1998) shifted the collocation point of each element forward to reduce the oscillation. Based on the existing work, Raven (1996) and Janson (1997) developed the fully nonlinear Rankine source method and achieved success on many full hull forms. Hess *et al.* (1980) applied higher order panels to the Rankine source method and improved the result of wave-resistance calculation.

Currently, the prevailing numerical methods of wave-making resistance are the Neumann-Kelvin method and the Rankine source method. Since the Rankine source method considers the nonlinear free surface boundary condition, theoretically it is more accurate than the Neumann-Kelvin method. However, the Neumann-Kelvin method only requires meshing on the ship hull surface, which is a typical practice in seakeeping analysis in the industry. The Rankine source method needs meshing both on the ship hull and the free surface. Both the hull surface and free surface need to be remeshed in every iteration. This brings difficulties in modeling and calculation. Moreover, Neumann-Kelvin methods can easily work with other Kelvin source method to solve wave-current coupling problems(e.g., Wang and Rogers (1989), Guha (2012), Guha and Falzarano (2015a, b)). All in all, there are pros and cons for these two methods, thus it is meaningful to test the limitations of these two methods. However, the published results about these two methods are limited. In this study, both methods were implemented and the wave-making resistance of a Wigley III hull and three Series 60 hulls (Cb=0.60, 0.70, 0.80) were calculated. By comparison of these two methods author tries to qualify the limitations of these two method.

Here is a brief introduction to this paper. The second section mainly describes the governing equations. Details of Kelvin source method are described in the third section. The fourth part describes the Rankine source method. The results of Wigley III and three Series 60 ships are given in the fifth section. Finally, the conclusions are given in the sixth section.

2. Governing equations

In this paper, the coordinate system moves with the ship and has the same speed, but it does not follow the trim and sinkage. The x axis points to the forward direction, the y axis points to port and the z axis points upward. The origin is at the midship.
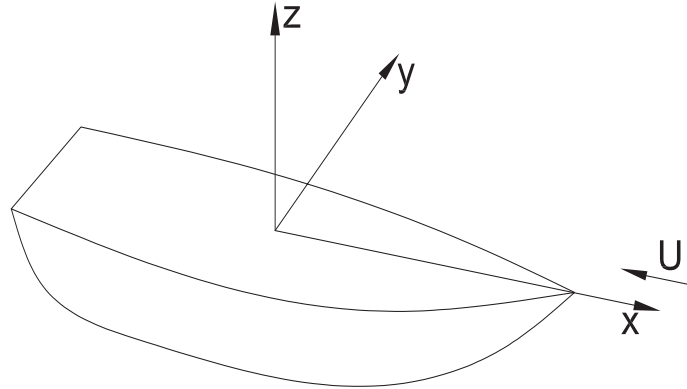
Fig. 1 Coordinate system

2.1 Gonverning equations of the total potential

In assumption of the ideal fluid, the fluid domain is an irrotational field. Φ is the velocity potential; η is the free surface elevation; (X, Y, Z) is any point in the fluid domain; U is the speed of the ship. The governing equations of the wave-making resistance problem are

Continuity

$$\nabla^2 \Phi = 0 \qquad (1)$$

The kinematic free surface boundary condition

$$\Phi_X \eta_X + \Phi_Y \eta_Y - \Phi_Z = 0 \quad at \quad Z = \eta(X, Y) \qquad (2)$$

The dynamic free surface boundary condition

$$\frac{1}{2}(U^2 - |\nabla\Phi|^2) - g\eta = 0 \quad at \quad Z = \eta(X, Y) \qquad (3)$$

The hull surface condition

$$\Phi_n = 0 \qquad (4)$$

$\vec{n}$ is the normal vector of the hull surface, as shown in Fig. 3.

The infinite depth condition

$$\Phi_Z = 0 \quad when \quad Z \to -\infty \qquad (5)$$

Additionally, there should be the radiation condition which guarantees that there are no waves ahead of the ship. Eqs. (1) to (5) together with the radiation condition are the governing equations of the wave-making problem.

2.2 Gonverning equations of the perturbation potential

In the study of wave-making problem, for the continence in study, the total velocity potential Φ is decomposed into the incoming flow potential $-UX$ and the perturbation potential ϕ

$$\Phi = -UX + \phi \tag{6}$$

Substitute Eq. (6) into Eq. (1) to Eq. (5). The governing equation in term of perturbation potential ϕ are

Continuity

$$\nabla^2 \phi = 0 \tag{7}$$

The kinematic free surface condition

$$(-U + \phi_X)\eta_X + \phi_Y \eta_Y - \phi_Z = 0 \quad on \quad Z = \eta(X, Y) \tag{8}$$

The dynamic free surface condition

$$\eta = \frac{1}{g}\left(U\phi_X - \frac{1}{2}|\nabla\phi|^2\right) \quad on \quad Z = \eta(X, Y) \tag{9}$$

The hull surface condition

$$\phi_n = U\cos(n, x) \tag{10}$$

The infinite depth condition

$$\phi_Z = 0 \quad Z \to -\infty \tag{11}$$

The radiation condition

$$\phi = \begin{cases} O\left(\dfrac{1}{\sqrt{X^2 + Y^2}}\right), X > 0, \sqrt{X^2 + Y^2} \to \infty \\ o\left(\dfrac{1}{\sqrt{X^2 + Y^2}}\right), X < 0, \sqrt{X^2 + Y^2} \to \infty \end{cases} \tag{12}$$

O denotes that $\dfrac{\phi}{\sqrt{X^2 + Y^2}} = 0$, and o denotes that $\dfrac{\phi}{\sqrt{X^2 + Y^2}} = 1$. The radiation condition guarantees there are no waves ahead of the ship bow.

Eqs. (7) to (12) are the governing equations of the wave-resistance problem in term of perturbation potential ϕ.

3. The Neumann-Kelvin method

3.1 Linearization of the free surface conditions

Expand the free surface conditions (8) and (9) on the calm water surface by Taylor expansion and keep the linear terms:

$$U\eta_X + \phi_Z = 0 \quad on \quad Z = 0 \tag{13}$$

$$\eta - \frac{U}{g}\phi_X = 0 \quad on \quad Z = 0 \tag{14}$$

Substitute Eq. (14) into Eq. (13), the combined free surface condition is

$$\phi_{XX} + K_0\phi_Z = 0 \quad on \quad Z = 0 \tag{15}$$

Where $K_0 = g/U^2$. Eqs. (7), (10), (11), (12) and (15) are the governing equations of the Neumann-Kelvin method.

3.2 Theintegralidentity

To reduce the number of freedom in the calculation, the surface panel method is used in the Neumann-Kelvin method. As shown in Figs. (2) and (3), assume there is a virtual fluid domain D_i inside of the hull surface; D_e is the fluid domain outside of the hull surface; ϕ^e is the velocity potential outside of the ship hull; ϕ^i is the velocity potential inside of the ship hull; S_{fe} is the free water surface outside of the ship hull; S_{fi} is the free water surface inside of the ship hull; S is the ship hull; S_{he} is the outside surface of ship hull; S_{hi} is the inside surface of ship hull; $\vec{n}$ is the normal vector pointing into the fluid domain; $\vec{n_e}$ is the normal vector of boundary of D_e. $\vec{n_i}$ is the normal vector of boundary of D_i.

In D_e, by Green's theorem(Brard 1972)

$$T\phi^e = \frac{1}{4\pi} \oiint_{S_{he}+S_{fe}} \left(\phi^e G_{n_e} - \phi^e_{n_e} G\right) dS \tag{16}$$

$\vec{X}$ is the coordinate of field point; $\vec{X_0}$ is the coordinate of source point. ϕ^e is supposed to be 0 on
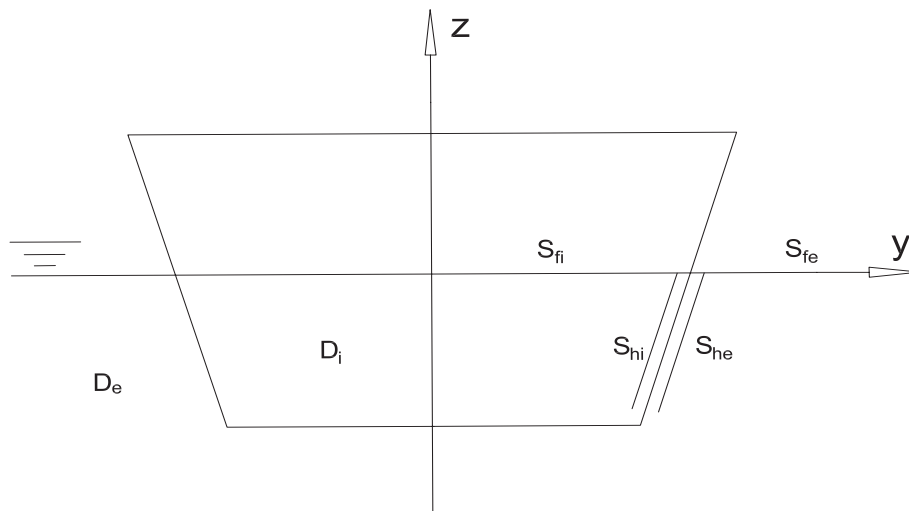

Fig. 2 Surfaces of different domains
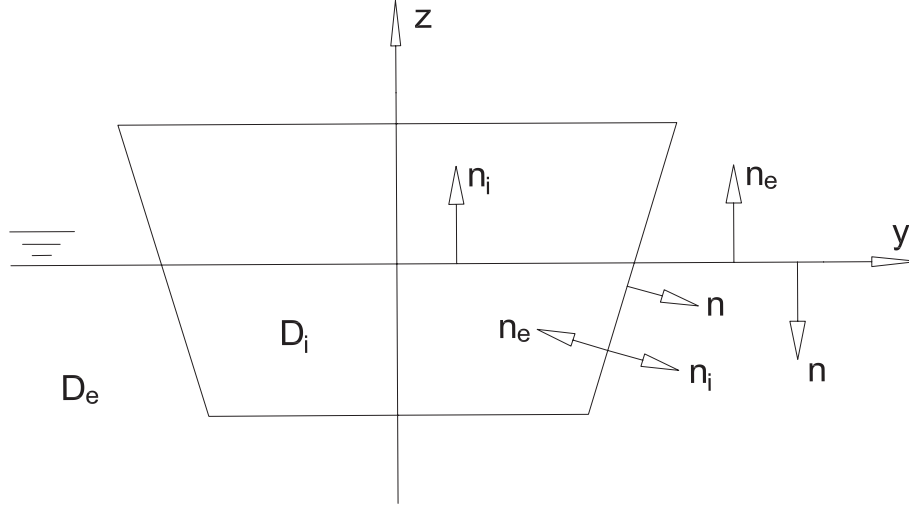
Fig. 3 Normal vectors of different domains

other boundaries of D_e.

$$
T = \begin{cases} 1 & when \quad \vec{X} \quad is \quad in \quad D_e \\ \frac{1}{2} & when \quad \vec{X} \quad is \quad on \quad S_h \\ 0 & when \quad \vec{X} \quad is \quad not \quad in \quad D_e \end{cases} \tag{17}
$$

Similarly,

$$
(1 - T)\phi^i = \frac{1}{4\pi} \oiint_{S_{hi}+S_{fi}} \left(\phi^i G_{n_i} - \phi^i_{n_i} G \right) dS \tag{18}
$$

Combine Eqs. (16) and (18). Since the S_{he} and S_{hi} are the same surface S_h with different normal vector, denote them as S_h. By Fig. (3), on hull surface: $\frac{\partial}{\partial n_i} = \frac{\partial}{\partial n}$, $\frac{\partial}{\partial n_e} = -\frac{\partial}{\partial n}$; on free water surface: $\frac{\partial}{\partial n_i} = -\frac{\partial}{\partial n}$, $\frac{\partial}{\partial n_e} = -\frac{\partial}{\partial n}$. In the whole fluid domain

$$
\begin{aligned}
\phi &= \frac{1}{4\pi} \iint_{S_h} \left\{ \left[\phi^e_n - \phi^i_n \right] G + \left[\phi^i - \phi^e \right] G_n \right\} dS \\
&+ \frac{1}{4\pi} \iint_{S_{fe}} \left[\phi^e_n G - \phi^e G_n \right] dS \\
&+ \frac{1}{4\pi} \iint_{S_{fi}} \left[\phi^i_n G - \phi^i G_n \right] dS
\end{aligned} \tag{19}
$$

On the free surface S_{fe} and S_{fi}, by the linear assumption of the Neumann-Kelvin method, $\frac{\partial}{\partial \vec{n}} \approx -\frac{\partial}{\partial Z}$, $dS \approx dXdY$. The surface integral can be changed to a double integral.

$$
\begin{aligned}
&\frac{1}{4\pi} \iint_{S_{fe}} \left(\phi^e_n G - \phi^e G_n \right) dS \\
&= \frac{1}{4\pi} \iint_{S_{fe}} \left(\phi^e G_Z - \phi^e_Z G \right) dXdY
\end{aligned} \tag{20}
$$

ϕ^e and G both satisfies the free surface boundary condition (15), substitute it into Eq. (20)

$$
\frac{1}{4\pi} \iint_{S_{fe}} \left(\phi^e G_Z - \phi^e_Z G \right) dX dY
$$

$$
= \frac{1}{4\pi K_0} \iint_{S_{fe}} \left(\phi^e_{XX} G - \phi^e G_{XX} \right) dX dY
$$

$$
= \frac{1}{4\pi K_0} \iint_{S_{fe}} \left[\left(\phi^e_{XX} G + \phi^e_X G_X \right) - \left(\phi^e G_{XX} + \phi^e_X G_X \right) \right] dX dY \tag{21}
$$

$$
= \frac{1}{4\pi K_0} \iint_{S_{fe}} \left[\left(\phi^e_X G \right)_X - \left(\phi^e G_X \right)_X \right] dX dY
$$

$$
= \frac{1}{4\pi K_0} \iint_{S_{fe}} \left(\phi^e_X G - \phi^e G_X \right)_X dX dY
$$

Using the Green's theorem

$$
\oint_L P dx + Q dy = \iint_D \left(\frac{\partial Q}{\partial x} - \frac{\partial P}{\partial y} \right) dx dy \tag{22}
$$

L is the boundary of D. Let $P = 0$

$$
\iint_D \frac{\partial Q}{\partial x} dx dy = \oint_L Q dy \tag{23}
$$
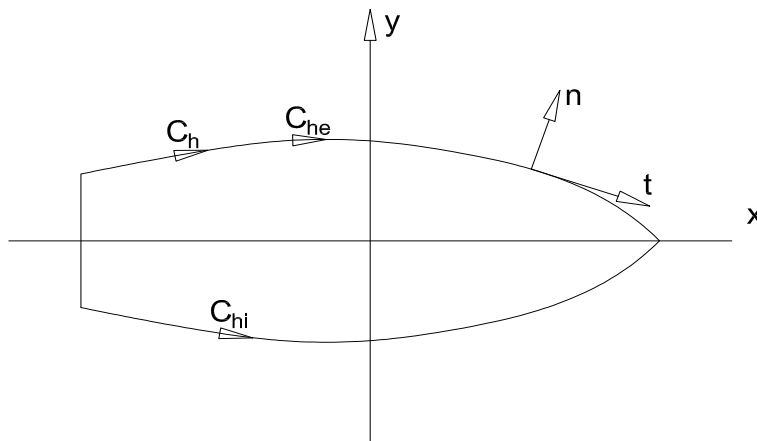
Fig. 4 Directions of the line integrals

Using Eq. (23)

$$\frac{1}{4\pi K_0} \iint_{S_{fe}} \left(\phi_X^e G - \phi^e G_X\right)_X dXdY$$
$$= \frac{1}{4\pi K_0} \oint_{C_{he}} \left(\phi_X^e G - \phi^e G_X\right) dY \tag{24}$$

By Eqs. (21) and (24)

$$\frac{1}{4\pi} \iint_{S_{fe}} \left(\phi_n^e G - \phi^e G_n\right) dS$$
$$= \frac{1}{4\pi K_0} \oint_{C_{he}} \left(\phi_X^e G - \phi^e G_X\right) dY \tag{25}$$

Similarly

$$\frac{1}{4\pi} \iint_{S_{fi}} \left[\phi_n^i G - \phi^i G_n\right] dS$$
$$= \frac{1}{4\pi K_0} \oint_{C_{hi}} \left(\phi_X^i G - \phi^i G_X\right) dy \tag{26}$$

Substitute Eqs. (25) and (26) into Eq. (19). By Fig. (4), $C_{he} = C_h$, $C_{hi} = -C_h$

$$\phi = \frac{1}{4\pi} \iint_{S_h} \left\{ \left[\phi_n^e - \phi_n^i\right] G + \left[\phi^i - \phi^e\right] G_n \right\} dS$$
$$+ \frac{1}{4\pi K_0} \oint_{C_h} \left\{ \left[\phi_X^e - \phi_X^i\right] G + \left[\phi^i - \phi^e\right] G_X \right\} dY \tag{27}$$

By Eq. (27), the point sources and dipoles are distributed both on the ship hull surface S_w and the waterline C_w. The source strength σ_s is

$$\sigma_s = \phi_n^e - \phi_n^i \tag{28}$$

The dipole strength is

$$m_d = \phi^i - \phi^e \tag{29}$$

The fluid inside of the ship hull surface is virtual, so ϕ^i can be chosen arbitrarily. If $\phi_n^i = \phi_n^e$, then σ_s is zero and only dipoles exist; if $\phi^i = \phi^e$, then m_d is zero and only point sources exist. If ϕ_i is other values, then it is the combination of point sources and dipoles. So the combination points sources and dipoles are not unique(Only point sources are used in this study, m_d is set to be zero later in the derivation(see Eq. (33)).

Set the local coordinate at any point on the waterline C_w. $\vec{n}$ is the normal vector pointing outside of the ship hull. $\vec{t}$ is tangent to C_w, $\vec{\tau}$ is vertical both to $\vec{n}$ and $\vec{t}$. The local coordinate system is shown in Fig. (4). Set

$$\alpha_t = \cos(X, t); \quad \alpha_\tau = \cos(X, \tau); \quad \alpha_n = \cos(X, n) \tag{30}$$

By Eqs. (28) to (30), in the local coordinate system on the waterline C_w

$$\phi_X^e - \phi_X^i = \sigma_s \alpha_n - \alpha_t \frac{\partial m_d}{\partial t} - \alpha_\tau \frac{\partial m_d}{\partial \tau} \tag{31}$$

Then substitute Eq. (28) to Eq. (31) into Eq. (27)

$$
\begin{aligned}
\phi = \frac{1}{4\pi} \iint_{S_h} (\sigma_s G + m_d G_n) dS + \frac{1}{4\pi K_0} \oint_{C_h} m_d G_X dY \\
+ \frac{1}{4\pi K_0} \oint_{C_h} \left(\sigma_s \alpha_n - \alpha_t \frac{\partial m_d}{\partial t} - \alpha_\tau \frac{\partial m_d}{\partial \tau} \right) G dY
\end{aligned}
\tag{32}
$$

Only the point sources are used in this study, set $m_d = 0$

$$
\phi = \frac{1}{4\pi} \iint_{S_h} \sigma_s G dS + \frac{1}{4\pi K_0} \oint_{C_h} \sigma_s \alpha_n G dY
\tag{33}
$$

By equation above, the sources are distributed on the hull surface and the waterline. Substitute Eq. (33) into Eq. (10). G contains the term $-1/|\vec{R}|$, $\vec{R} = \vec{X} - \vec{X_0}$. When $\vec{X} \to \vec{X_0}$, $-1/|R|$ is $0/0$. Use a hemisphere to remove this singularity, as shown in Fig. (5).

$$
\begin{aligned}
\lim_{\varepsilon \to 0} \iint_\varepsilon \frac{\partial}{\partial n} \left(-\frac{1}{R} \right) \sigma_s dS \\
= \lim_{\varepsilon \to 0} \iint_\varepsilon \frac{\partial}{\partial R} \left(-\frac{1}{R} \right) \sigma_s dS \\
= 2\pi \sigma_s
\end{aligned}
\tag{34}
$$

Substitute Eqs. (33) and (34) into Eq. (10)

$$
\begin{aligned}
\frac{1}{2}\sigma_s + \frac{1}{4\pi} \iint_{S_h} \sigma_s G_n dS + \frac{1}{4\pi K_0} \oint_{C_h} \alpha_n \sigma_s G_n dy \\
= U \cos(n, x)
\end{aligned}
\tag{35}
$$
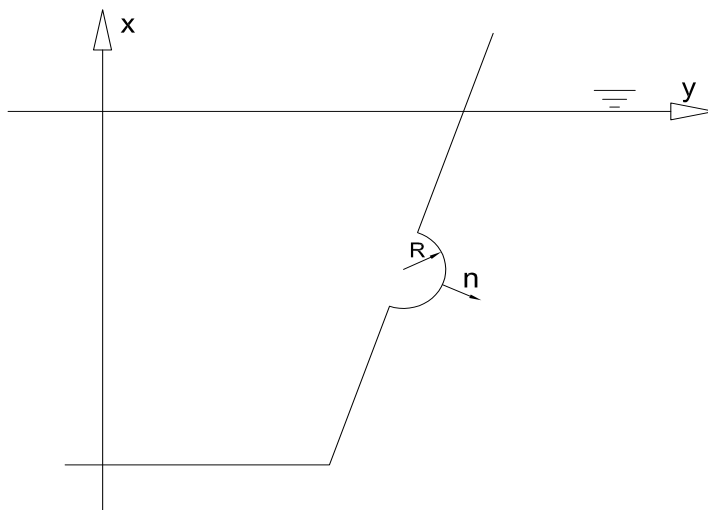
Fig. 5 Removal of the singularity

Eq. (35) is the integral identity of the Neumann-Kelvin method. It is satisfied on the hull surface. If the Green's function is known, the only unknown variable is σ_s. In this study, the hull surface is discretized into flat panels and the source strength is a constant in every panel. Eq. (35) is satisfied on one point in every panel, which is called the collocation point. The waterline is also discretized and set the source strength of the waterline the same with the source strength of the panel in which the waterline belongs to. The number of unknown variable is the same with the number of equations. This study mainly used rectangular panels in the meshing and some triangular panels were also used for the continence of modeling. The mesh on the hull surface is shown in Fig. (6).

3.3 The Green function

The Green function for the wave-making resistance problem is determined by coordinates of the source and field points, the velocity of fluid U, and the wave number g/U^2. Then normalize the coordinates of source and field point by the wave number. As a result of the normalization, the Green's function only relies on relative position of source and field points. Using the coordinates defined above, the Green's function can be written in the form(Wehausen and Laitone 1960)

$$
\begin{aligned}
G = &-\frac{1}{r_0} + \frac{1}{r} \\
&+ \frac{4}{\pi} \int_0^{\pi/2} d\theta \fint_0^{\infty} dk \frac{e^{kz} \cos(kx\cos\theta)\cos(ky\sin\theta)}{k\cos^2\theta - 1} \\
&+ 4 \int_0^{\pi/2} d\theta e^{z\sec^2\theta} \sin(x\sec\theta)\cos(y\sec^2\theta\sin\theta)\sec^2\theta
\end{aligned}
\tag{36}
$$
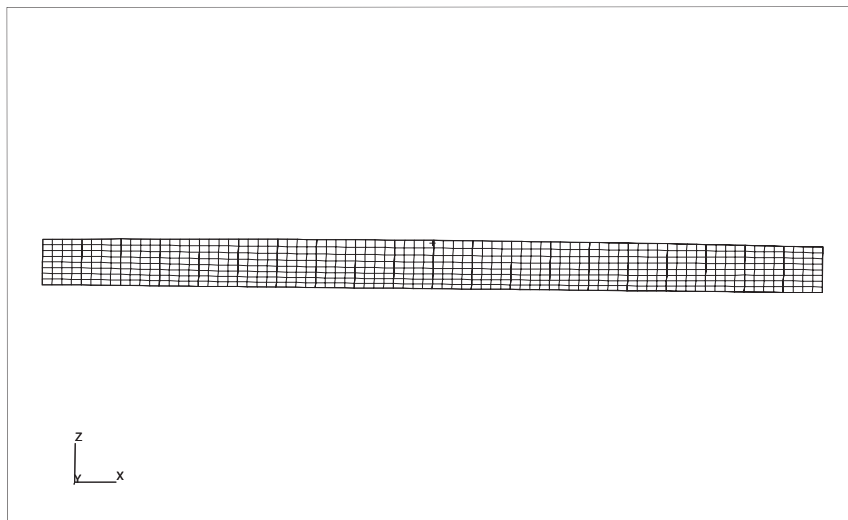
Fig. 6 Mesh on the hull surface

where

$$(x_1, y_1, z_1) = \frac{g}{U^2}(X_1, Y_1, Z_1) \tag{37}$$

$$(x_0, y_0, z_0) = \frac{g}{U^2}(X_0, Y_0, Z_0) \tag{38}$$

$$(x, y, z) = (x_1 - x_0, y_1 - y_0, z_1 + z_0) \tag{39}$$

$$r_0 = \sqrt{(x_1 - x_0)^2 + (y_1 - y_0)^2 + (z_1 - z_0)^2} \tag{40}$$

$$r = \sqrt{(x_1 - x_0)^2 + (y_1 - y_0)^2 + (z_1 + z_0)^2} \tag{41}$$

(X_1, Y_1, Z_1) is the dimensional coordinate of the field point; (X_0, Y_0, Z_0) is the dimensional coordinate of the source point; r_0 is the distance between the field and source points; r is the distance between field and the image of the source point above the xy plane. $\fint$ denotes the principle value of the integral.

The Green function can be divided into three parts:

1. $R = -\dfrac{1}{r_0} + \dfrac{1}{r}$, the Rankine source term, which denotes the potential of point source in an infinite fluid domain.

2. $D = \dfrac{4}{\pi} \int_0^{\pi/2} d\theta \int_0^\infty dk \dfrac{e^{kz} \cos(kx \cos\theta) \cos(ky \sin\theta)}{k \cos^2\theta - 1}$, the double integral term, which denotes the near-field potential of the source. D is non-oscillatory and symmetric in x and y directions.

3. $W = 4 \int_0^{\pi/2} d\theta e^{z \sec^2\theta} \sin(x \sec\theta) \cos(y \sec^2\theta \sin\theta) \sec^2\theta$, the single integral term, which denotes the far-field potential of the source. W is a wavelike disturbance which represents waves generated by translating point source.

The following subsections will discuss the calculation of the Green function.

3.4 The Rankine source potential

R includes two terms, $-\dfrac{1}{r_0}$ and $\dfrac{1}{r}$, which represent the potential of a point source and its image source in an infinite fluid domain. Hess and Smith (1962, 1967) in their remarkable work gave results of the potential and velocity generated by point sources distributed on quadrilateral panels. Their results were used to calculate the Rankine source part R.

3.5 The nearfield potential

D is the double integral part of the Green's function. It can be calculated by the sum of Chebyshev series and a singularity(Newman 1987, Eq. 48)

$$D \approx S + \sum_{i=0}^{16} \sum_{j=0}^{16} \sum_{k=0}^{18} P_{ijk}[f(R)]^i \left(-1 + \frac{4}{\pi}\theta\right)^j \left(\frac{2}{\pi}\alpha\right)^{2k} \tag{42}$$

(R, θ, α) is the spherical coordinates, where

$$R = \sqrt{x^2 + y^2 + z^2}; \quad \theta = \arctan\left(\frac{x}{\sqrt{y^2 + z^2}}\right)$$

$$\alpha = \arctan\left(\frac{y}{z}\right) \tag{43}$$

$f(R)$ is a function of R

$$f(R) = \begin{cases} 2R & (0 < R \le 1) \\ (2R - 5)/3 & (1 \le R \le 4) \\ (R - 7)/3 & (4 \le R \le 10) \\ 1 - 20/R & (10 \le R \le \infty) \end{cases} \tag{44}$$

Coefficients P_{ijk} are given in four tables by Newman (1987). S is the term to remove singularity near origin(Newman 1987, Eq. 21)

$$\begin{aligned} S = & -U_1 + zU_3 - yV_3 - xU_2 \\ & + \frac{1}{2}[-z^2 U_5 + y^2(U_3 + U_5) - x^2 U_3] \\ & + yzV_5 + xzU_4 - xyV_4 \\ & + \frac{1}{6}[z^3 U_7 + y^3(V_5 + V_7) - x^3 U_4] \\ & + \frac{1}{2}[-z^2 yV_7 - z^2 xU_6 - y^2 z(U_5 + U_7) \\ & + y^x(U_4 + U_6) + x^2 zU_5 - x^2 yV_5] + xyzV_6 \end{aligned} \tag{45}$$

Where

$$U_m = \frac{2i^m}{\pi} \int_{-\frac{\pi}{2}}^{\frac{\pi}{2}} \cos^m \theta \log(\upsilon) d\theta \tag{46}$$

$$V_m = \frac{2i^m}{\pi} \int_{-\frac{\pi}{2}}^{\frac{\pi}{2}} \cos^{m-1} \theta \sin \theta \log(\upsilon) d\theta \tag{47}$$

$$\upsilon = z \cos^2 \theta - y \cos \theta \sin \theta + i|x| \cos \theta \tag{48}$$

U_m and V_m are still in the integral form. To improve the calculation efficiency, V_m terms can be calculated by trigonometric series(Newman 1987, Eq. 27)

$$V_m = \frac{2^{2-m}}{m} \sum_{k=0}^{[\frac{1}{2}m - \frac{1}{2}]} C_k^m (-1)k \sin[(m - 2k)\alpha]\left(\frac{\rho}{R + x}\right)^{m-2k} \tag{49}$$
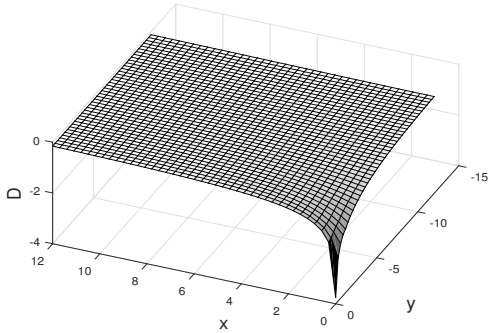
Fig. 7 Value of $D(x, y, z)$ when $z = -0.1$
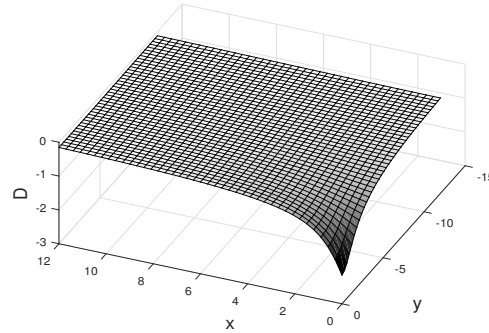
Fig. 8 Value of $D(x, y, z)$ when $z = -1.0$
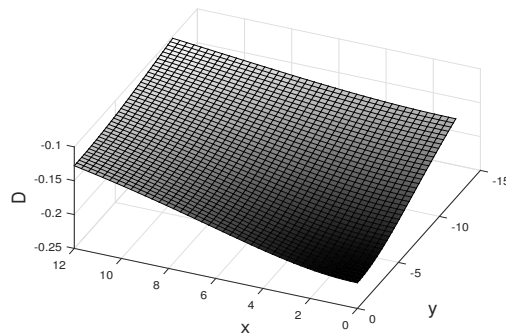
Fig. 9 Value of $D(x, y, z)$ when $z = -10.0$

U_m can be calculated by iterative formula

$$
\begin{aligned}
& mU_m + (m-1)U_{m-2} \\
& 2i^m \frac{1 \cdot 1 \cdot 3 \cdot ... \cdot (m-3)}{2 \cdot 4 \cdot 6 \cdot ... \cdot (m)} - \frac{2^{2-m}}{2} \\
& \cdot \sum_{k=0}^{\left[\frac{1}{2}m - \frac{1}{2}\right]} C_m^k (-1)^k (m-2k) \cos[(m-2k)\alpha] \left(\frac{\rho}{R+x}\right)^{m-2k}
\end{aligned}
\tag{50}
$$

$$
U_0 = 2\log\left(\frac{R+x}{4}\right)
\tag{51}
$$

Γ is the gamma function

$$
\Gamma(n) = (n-1)!
\tag{52}
$$

n is a positive integer. The double integral term D can be calculated by Eq. (42) to Eq. (52). The results are shown in Figs. (7) to (9). By these results, it is clear that D only has effect on the fluid domain which is near the point source. The influence of D decays rapidly when the field point is far away from the source point. So D presents the near-field influence of the point source in the fluid domain.
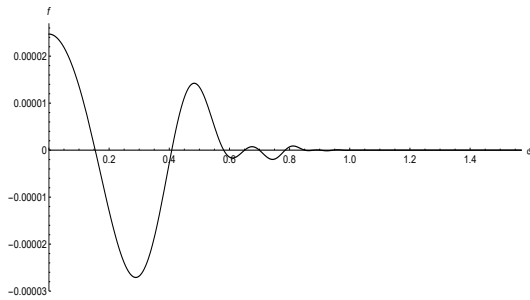
Fig. 10 f when $x = -10, y = 10, z = -5$
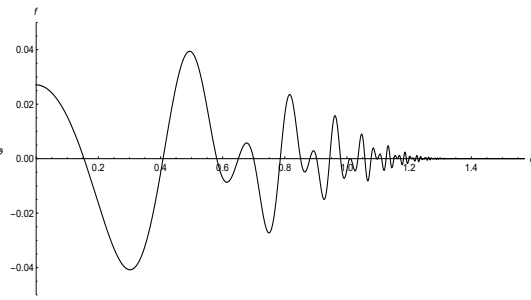
Fig. 11 f when $x = -10, y = 10, z = -1.5$
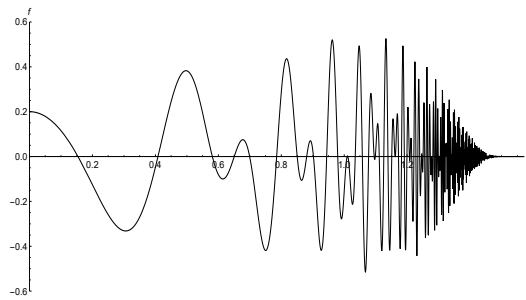
Fig. 12 f when $x = -10, y = 10, z = -0.5$

3.6 The far-field potential

W is the single integral part of the Green's function. Calculation of W is difficult since the integrand oscillates severely, especially when $z \to 0$. Define f as the integrand of W

$$f = e^{z \sec^2 \theta} \sin(x \sec \theta) \cos(y \sec^2 \theta \sin \theta) \sec^2 \theta \tag{53}$$

f is shown in Fig. (10) to Fig. (12).

From the results we can see that f is increasingly oscillatory when z goes close to 0. Both the frequency and amplitude grows fast when $z \to 0$. For this reason, the calculation of W only has very low efficiency by the routine numerical integration method(e.g., the Simpson method).

Numerical integration

Due to the oscillatory behavior of the integrand, W can not be calculated by the routine integration method. One idea is to change the integrand into a less oscillatory one. The steepest descend method is used in this study. W can be written in the form

$$W = 2Im(I(x, y, z) + I(x, -y, z)) \tag{54}$$

where

$$I(x, y, z) = \int_0^\infty e^{\omega(x,y,z,t)} dt \tag{55}$$

$$\omega(x, y, z, t) = z(1 + t^2) + i(x - yt)\sqrt{1 + t^2} \tag{56}$$

By Jordan's lemma and the steepest descend method(Motygin 2014), change the integral path $t \rightarrow e^{i\theta}t$

$$I(x, y, z) = \int_0^{t_*} e^{\omega(x,y,z,t)}dt + e^{i\theta} \int_0^{\infty} e^{\omega(x,y,z,t_* + te^{i\theta})}dt \tag{57}$$

where

$$\cos 2\theta = \frac{-z}{\sqrt{y^2 + z^2}}, \quad \sin 2\theta = \frac{-y}{\sqrt{y^2 + z^2}} \tag{58}$$

$$\cos \theta = \sqrt{\frac{1 + |z|/\sqrt{y^2 + z^2}}{2}} \tag{59}$$

$$\sin \theta = sign(-y)\sqrt{\frac{1 - |z|/\sqrt{y^2 + z^2}}{2}} \tag{60}$$

$$t_* = \frac{|x|\sin\theta}{2(|z|\cos\theta - y\sin\theta)} \tag{61}$$

The two integrals in Eq. (57) can be transformed into integrals on $[-1, 1]$

$$\int_0^{t_*} g(t)dt = \frac{t_*}{2}\int_{-1}^1 g\left(\frac{t_*(t+1)}{2}\right)dt = \int_{-1}^1 f(t)dt \tag{62}$$

$$\int_0^{\infty} g(t)dt = 2\int_{-1}^1 \frac{1}{(1-t)^2}g\left(\frac{t+1}{1-t}\right)dt = \int_{-1}^1 f(t)dt \tag{63}$$

An efficient method to calculate the integral $\int_0^1 f(t)dt$ is by the Clenshaw-Curtis quadrature(Gentleman 1972).

$$\int_{-1}^1 f(t)dt = d_0 + 2\sum_{k=1}^{\infty} \frac{d_k}{1 - (2k)^2} \tag{64}$$

where

$$d_k = \frac{2}{\pi}\int_0^{\pi} f(\cos\theta)\cos(2k\theta)d\theta \tag{65}$$

d_k can be calculated by the trapezoidal rule

$$d_k \approx \frac{2}{N}\left[\frac{f(1)}{2} + \frac{f(-1)}{2} + \sum_{n=1}^{N-1} f(\cos(\frac{n\pi}{N}))\cos(\frac{2\pi nk}{N})\right] \tag{66}$$

W can be calculated by Eq. (54) to Eq. (66).

The functional method

The other way to calculate the single integral term W is by functional series. W can be expressed by two Bessel's series(Bessho 1964)

When $\frac{x}{\sqrt{\rho}}$ is small

$$W = -2e^{\frac{z}{2}}\sum_{n=0}^{\infty}(-1)^n\varepsilon_n K_n(\frac{1}{2}\rho)\acute{J}_{2n}(x)\cos(n\alpha) \tag{67}$$

Table 1 A combination of two methods in calculation of far-field disturbance

	$-0.3 < z < 0$	$z < -0.3$
$x < 8\sqrt{y}$		Bessho's series (Eq. 67)
$8\sqrt{y} < x < 12\sqrt{y}$	The steepest descend method	The steepest descend method
$x > 12\sqrt{y}$		Bessho's series (Eq. 68)

When $\frac{x}{\sqrt{\rho}}$ is large

$$W = 2\pi e^{\frac{z}{2}} \sum_{n=0}^{\infty} \varepsilon_n I_n(\frac{1}{2}\rho) \acute{Y}_{2n}(x) \cos(n\alpha) \tag{68}$$

where

$$\rho = y^2 + z^2, \quad \alpha = tan^{-1}(\frac{y}{z}) \tag{69}$$

$$\varepsilon_n = \begin{cases} 1 & n = 1 \\ 2 & n \geq 2 \end{cases} \tag{70}$$

There is an additional term which is missing from the Bessho's series(Ursell 1960) and this term makes the two Bessho's series truely complementary. However, this missing term is only effective near the *xy* plane. In this study, the Bessho's function will not be used near the free surface, so this additional term will not be discussed here.

A combination of the two methods

In this study, a combination of the numerical integration and the Bessho's series is used to calculate W. In the domain near the *xy* plane and in the transformed area of two Bessho's series, the numerical integral is used. Bessho's series is used in the rest of the fluid domain. The detailed algorithm is shown in Table (1).

The results of W are shown in Fig. (13) to Fig. (15). Fig. (13) shows that the value of W oscillates much when $z \to 0$, thus the accurate numerical integral method should be used in this domain. As z grows, the oscillation decays as value of z grows. When $z = -1.0$, both the numerical integration and Bessho's series are used. By Fig. (15), the value of W is continuous. These two method give the same result in the domain far away from the *xy* plane.

4. The Rankine source method

4.1 Free surface boundary condition

In the Rankine source method, the free surface boundary conditions are linearized on a base flow. Set

$$\Phi = \psi + \varphi \tag{71}$$

$$\eta = H + \xi \tag{72}$$
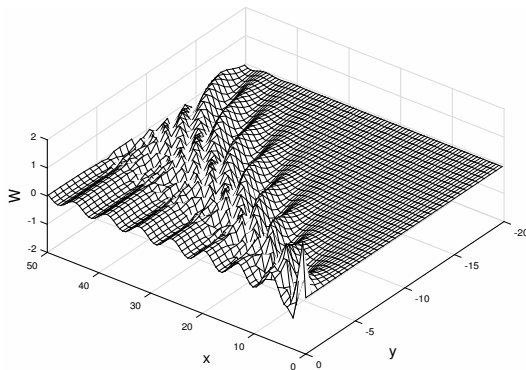
Fig. 13 Value of *W* when z=-0.1
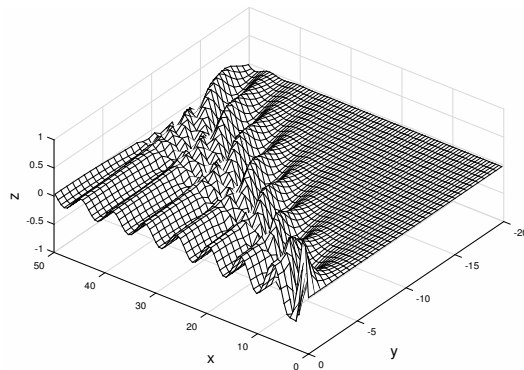
Fig. 14 Value of *W* when z=-0.3
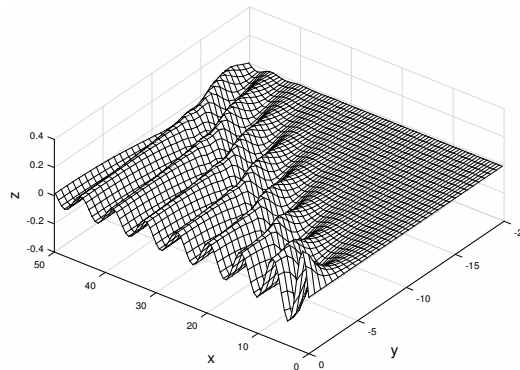
Fig. 15 Value of *W* when z=-1.0

ψ and H are the potential and wave elevation of the base flow, φ and ξ refer to the perturbation flow.

Substitute Eqs. (71) and (72) into Eqs. (2) and (3) and keep the linear terms about the perturbation flow.

$$\psi_X\eta_X + \psi_Y\eta_Y + \varphi_X H_X + \varphi_Y H_Y - \psi_Z - \varphi_Z = 0 \tag{73}$$

$$\frac{1}{2}[U^2 - \nabla\psi \cdot \nabla\psi - 2\nabla\psi\nabla\varphi] - g\eta = 0 \tag{74}$$

Substitute Eq. (74) to Eq. (73). The combined free surface condition is

$$\begin{aligned}
&\frac{1}{2}(\psi_X\frac{\partial}{\partial X} + \psi_Y\frac{\partial}{\partial Y})[\psi_X^2 + \psi_Y^2 + \psi_Z^2 + 2\psi_X\varphi_X + 2\psi_Y\varphi_Y \\
&+ 2\psi_Z\varphi_Z] - g(\varphi_X H_X + \varphi_Y H_Y) + g(\psi_Z + \varphi_Z) = 0 \\
&on \quad z = H(x, y)
\end{aligned} \tag{75}$$

4.2 The integral identity

S is surface composed of the free surface and the hull surface; D_I is the virtual fluid domain; D_E is the fluid domain; ϕ^I is the perturbation potential in D_I; ϕ^E is the perturbation potential in D_E. Different from the Neumann-Kelvin method, the virtual domain D_I has no free surface and denotes

the whole domain above S. $\vec{X}$ is the field point; $\vec{X_0}$ is the source point. The normal vectors of different domain are as shown Fig. (16).

By the Green's theorem

$$t\phi^I = \frac{1}{4\pi} \iint_S \left(\phi^I G_{n_I} - G\phi^I_{n_I} \right) dS \tag{76}$$

Since ϕ is the perturbation potential, the integral on other boundaries is 0.

$$t = \begin{cases} 1 & when & \vec{X} & is & in & D_I \\ \frac{1}{2} & when & \vec{X} & is & on & S \\ 0 & \vec{X} & is & in & D_E \end{cases} \tag{77}$$

Similarly

$$(1 - t)\phi^E = \frac{1}{4\pi} \iint_S \left(\phi^E G_{n_E} - G\phi^E_{n_E} \right) dS \tag{78}$$

By Fig. (16), on S

$$\frac{\partial}{\partial n} = -\frac{\partial}{\partial n_E} = \frac{\partial}{\partial n_I} \tag{79}$$

Combine Eq. (76) and Eq. (78), consider Eq. (79)

$$\phi = \frac{1}{4\pi} \iint_S \left[(\phi^I_n - \phi^E_n)G + (\phi^E - \phi^I)G_n \right] dS \tag{80}$$

By Eq. (80), we can see there is sources and dipoles distributed on S. Since the fluid domain D_E is virtual, ϕ^E can be set to $\phi^E = \phi^I$. So the velocity potential is continuous on S.

$$\phi = \frac{1}{4\pi} \iint_S \sigma G dS \tag{81}$$

σ is the source strength

$$\sigma = \phi^I_n - \phi^E_n \tag{82}$$
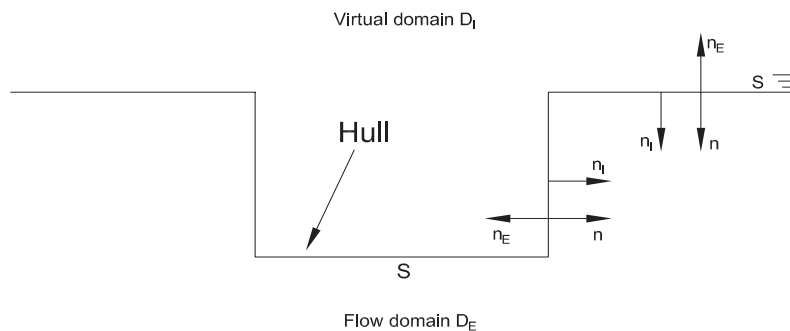
Fig. 16 Normal vectors in the Rankine source method

Substitute Eq. (6) into Eq. (82)

$$\Phi = -UX + \frac{1}{4\pi} \iint_S \sigma G dS \tag{83}$$

Substitute Eq. (83) into Eqs. (4) and (75) and the source strength σ can be calculated. In numerical calculation, S is discretized into flat panels and the source strength is a constant in every panel. The mesh in the Rankine source method is shown in Fig. (17).

In Eq. (83), S is the whole free water surface. L is the ship length. In numerical calculation, the panels can only cover part of the free surface. In this study. panels cover the free surface which is L ahead of the bow, L behind the stern and L in width. The free surface elevation varies severely near the ship hull and decays far away the ship hull. For this reason, the panels are dense near the ship hull and relative sparse far away the ship hull. The distribution of the mesh seeds in y direction is a geometric sequence and the coefficient is $b_2/b_1 = 1.1$, as shown in Fig. (18).

4.3 The forward shift of the allocation point

In the Rankine source method, the source strength over one panel is a constant and the boundary condition is satisfied on one point which is called the allocation point. For intuition the allocation should be the geometry center. However, calculated source strength oscillates severely for this choice. That is to say, the calculated result of the source strength varies severely between the nearby panels(Raven 1998). This is the sign of error in the numerical calculation. One method to solve this is to move the allocation point ahead of the geometry center, as shown in Fig. (18). By this method, the result of the source strength is continuous over the nearby panels. Since the location of the allocation point can be chosen freely over the panel, the forward shift of the allocation point would not introduce extra error in the calculation. The prove of the effectiveness of this method is give by
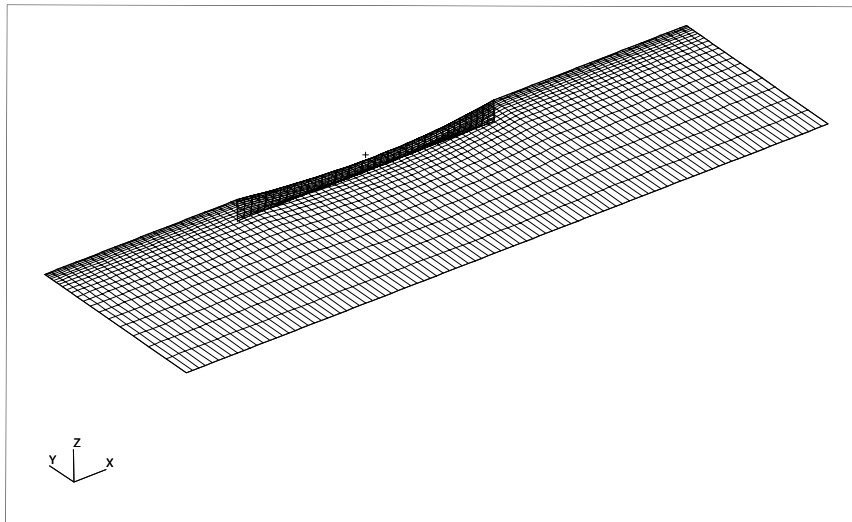

Fig. 17 Mesh in the Rankine source method
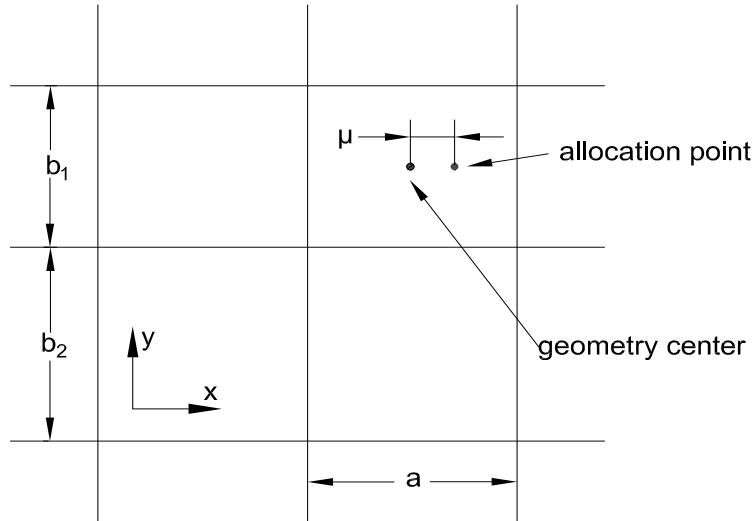
Fig. 18 Forward shift of the allocation point

Raven (1998). In this study, the distance between the allocation point and the geometry center is 10% of the panel length, $\mu = 0.1a$, as shown in Fig. (18).

4.4 The raised panel method

In the Rankine source method, the discretization of source strength and the use of difference scheme in the boundary condition introduce the numerical wave dispersion(Han and Olson 1987b, Schultz and Hong 1989b). That is to say, the calculated wave length is different from the actual wave length. To reduce the wave dispersion, the panels are above the free surface at some distance, which
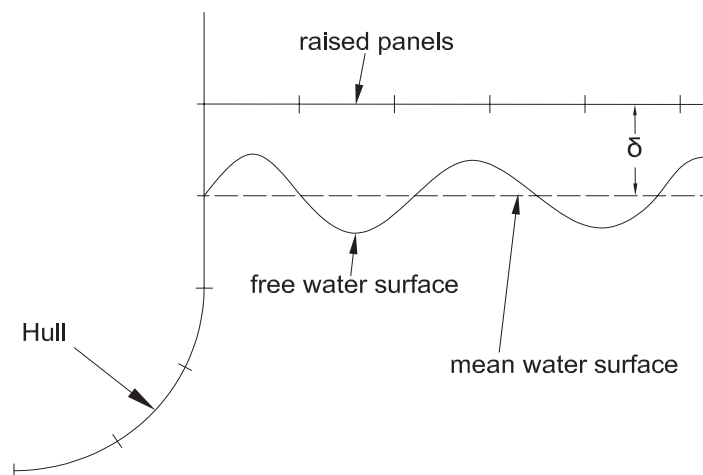
Fig. 19 The raised panel method

is called the raised panel method. The effectiveness of this method is given by Musker (1989) and Cao (1991b). In the Rankine source method, the free surface elevation varies in every iteration. So the free surface should be remeshed in every iteration. In the raised panel method, the panels are above the free surface and the calculated result is not sensitive to the distance of panels above the free surface(Raven 1996). So the free surface does not need to be remeshed in every step. This can bring much convenience in calculation and this is another advantage of the raised panel method. The panels should not be too close to the free surface since the effect of the raised panel method is too weak to reduce the wave dispersion. The panels should not be too far away from the free surface either since this would cause the singularity in the calculation. In this study, the panels are above the free surface 15% of the panel length, $\delta = 0.15a$, as shown in Fig. (19).

4.5 The difference scheme

The boundary conditions requires the derivative of velocity. The forward difference scheme in x direction can introduce virtual frictional force and thus satisfy the radiation condition(Dawson 1977). The result of calculation is not sensitive to the choice of the difference scheme(Raven 1996). In this study, four point forward scheme is used in x direction

$$\frac{\partial f}{\partial x} \approx \frac{10 f_{i,j} - 15 f_{i-1,j} + 6 f_{i-2,j} - f_{i-3,j}}{6 \Delta x} \tag{84}$$

Central scheme is used in y direction

$$\frac{\partial f}{\partial y} \approx \frac{f_{i,j+1} - f_{i,j-1}}{2 \Delta x} \tag{85}$$

4.6 Initial conditions

In the derivation of the Rankine source method, there is no restriction on the initial condition. In practice, often a uniform ship speed and calm water free surface are chosen. However, for highly nonlinear cases(e.g., the Froude number is very large), the simple initial conditions may lead to divergence of the result. For these highly nonlinear cases, the choice of initial conditions is important. The principle is to choose the initial conditions which are close to the (expected) final result, for example, choose the initial conditions as the result from Dawson's method. This is in accordance with the assumptions of the perturbation method. From Eqs. (71) and (72), φ and ξ should be small variables compared with ψ and H.

4.7 The convergence criteria

By the free surface boundary condition (75)

$$g(\varphi_Z - \varphi_X H_X - \varphi_Y H_Y) + (\psi_X \frac{\partial}{\partial X} + \psi_Y \frac{\partial}{\partial Y})$$

$$(\psi_X \varphi_X + \psi_Y \varphi_Y + \psi_Z \varphi_Z) \tag{86}$$

$$= -g \epsilon_k + (\psi_X \frac{\partial}{\partial X} + \psi_Y \frac{\partial}{\partial Y}) \epsilon_d \quad on \quad Z = H(X, Y)$$

Where

$$\epsilon_k = \psi_Z - \psi_X H_X - \psi_Y H_Y \tag{87}$$
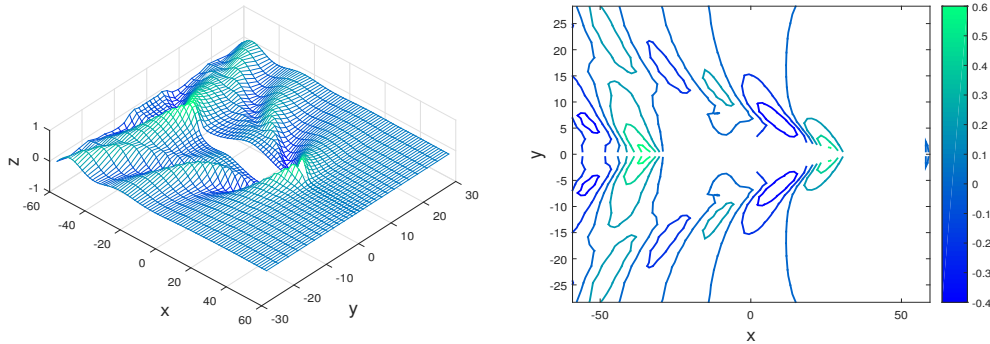
Fig. 20 Wave elevation and contour of Wigley III, $F_n = 0.3$

$$\epsilon_d = \frac{1}{2}(U^2 - \psi_X^2 - \psi_Y^2 - \psi_Z^2) - gH \tag{88}$$

Set $\epsilon_k = \epsilon_d = 0$ be the convergence criteria. This can be explained physically and mathematically. Mathematically, when ϵ_d and ϵ_k are both 0, then the right hand side of equation is 0. Since Eq. (86) is satisfied on the whole free surface $Z = H(X, Y)$, by the left hand side of Eq. (86), $\varphi_x = \varphi_y = \varphi_z = 0$. As ϕ is the disturbance potential, this means the algorithm is convergent. Physically, from Eqs. (87) and (88), $\epsilon_k = \epsilon_d = 0$ means that ψ and H satisfy the kinematic and dynamic free surface boundary condition, which implies that ψ and H are already the convergent solution.

In every iteration, calculate ϵ_k and ϵ_d on every panel on the free surface. Then the convergence criteria is

$$(\epsilon_k)_{max} < aU \tag{89}$$

$$(\epsilon_d)_{max} < bU^2 \tag{90}$$

a and b are chosen as constants, usually $a = b = 0.005$.

In this study, the Rankine source is implemented and the calculated free surface elevation and contour are shown in Fig. (20).

5. Comparision of the Neumann-Kelvin and Rankine source methods

To compare the Neumann-Kelvin and Rankine source method, and to explore the limitations of these two methods, both methods were implemented and the wave-making resistance of a Wigley III ship and three Series 60(Cb=0.6, 0.7, 0.8) ships were calculated by both methods. The results were compared to the experimental results. In the calculation, for the Neumann-Kelvin source method, approximately 2000 elements were used for the ship hull surface; for the Rankine source method, approximately 2000 elements were used for the ship hull surface and 6000 elements were used for the free surface. The results are shown in Fig. (21)

The calculated results by two methods were compared with experiment results from DTMB(Todd 1963). Only the total drag coefficients were given by the experiments and the wave-making coefficients were calculated by the three-dimensional transform(Lewis 1988). The result of Wigley III was also compared with the calculated result by Marr (1996). For the Wigley III and Series 60(Cb=0.6)

(a) Wigley III

(b) Series 60, Cb=0.6

(c) Series 60, Cb=0.7
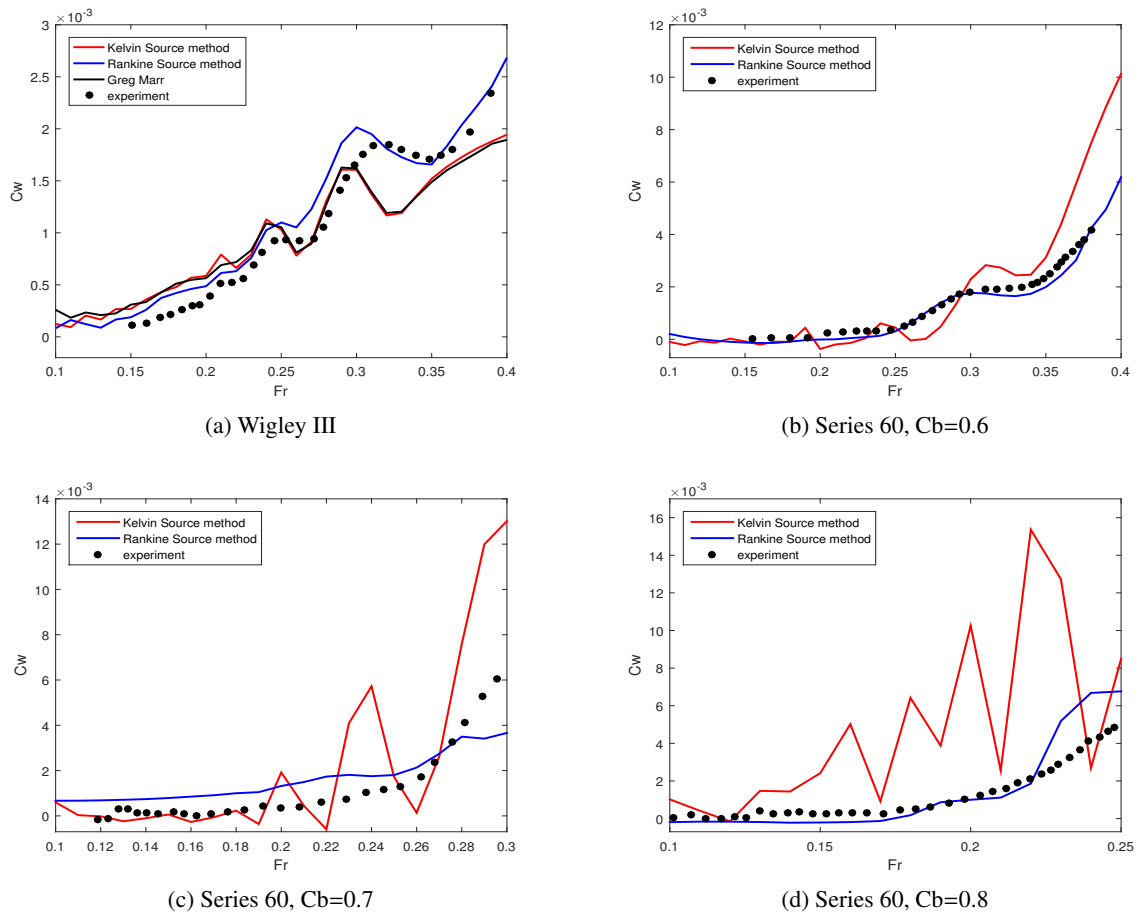
(d) Series 60, Cb=0.8

Fig. 21 Comparision of the Neuman-Kelvin and the Rankine source method on four ships

ship, the results were shown for Froude number $Fn = 0.1 \sim 0.4$. For the Series 60(Cb=0.7,0.8) ship, the results were shown for shorter range of Froude number due to the lack of experiment data for the high Froude number. This is reasonable because Series 60(Cb=0.7,0.8) ship are full form ships. When the Froude number is too high, wave breaking would appear in the experiment, which is not considered in the potential theory. Moreover, the full form ship usually can not travel at a high Froude number in actual use.

From the results we can see that the Neumann-Kelvin method can yield relative good result for the Wigley III ship(compared to the series 60 ships), especially when the Froude number is small. But it gives unrealistic results of wave-making resistance for the series 60 ships. As the block coefficient grows, the curve of wave-making resistance begins to oscillate at a lower Froude number and oscillates more severely. This is because the Wigley III is an idealized hull form and somewhat like the thin ship. The waves generated by the ship are close to the linear waves. However, the Series 60 ships are more realistic ship hulls. As the block coefficient of hull forms grows, the waves generated by the ship are highly nonlinear at a lower Froude number. This violate the basic

assumption of the Neumann-Kelvin method.

Compared to the Neumann-Kelvin method, the Rankine source method gives much more satisfactory result for Wigley III and all three Series 60 ship hulls. Unlike the Neumann-Kelvin method, the Rankine source method uses nonlinear free surface condition. So as the block coefficient and the Froude number grows, the Rankine source method can still satisfy the highly nonlinear free surface boundary condition. However, For the Series 60(Cb=0.7,0.8) ships, when the Froude number is high, the Rankine source generates large error. This may caused by the direct pressure integral over the hull surface in the calculation. Since the pressure on the fore half and rear half of the ship hull is opposite, the wave-making resistance is the subtraction of two large numbers. This may cause numerical errors in the calculation. One possible solution is by the wave cut analysis, which is discussed by the author's another paper(Yu and Falzarano 2017).

6. Conclusions

In this study, two methods of calculating wave-making resistance were explored. The first method is the Neumann-Kelvin method, which assumes the linear free surface condition. The key point of the Neumann-Kelvin method is to calculate the Green function, especially the single integral part. In this study, the derivation of the integral identity and the method to calculate the Green function were discussed.

The second method of calculating wave-making resistance is the Rankine source method, which uses the nonlinear free surface condition. The raised panel method and the shift of collocation point were used in this study. The integral identity, initial conditions, and convergence criteria were also discussed in this paper.

In this study both the Neumann-Kelvin and the Rankine source method were implemented and the wave-making resistance of a Wigley III ship and three Series 60 (Cb=0.6,0.7,0.8) ships were calculated. The Neumann-Kelvin method can only give satisfactory result for Wigley III ship but the Rankine source method can give much more reasonable results for all ships. The main difference of the results is due to the treatment of free surface boundary condition. This study denotes that the free surface boundary condition is very important to problem of wave-making resistance. Based on the results of this paper, the Rankine source method is more accurate in the calculation of the wave-making resistance. However, the Neumann-Kelvin method is much more convenient in modeling since it only needs to mesh the ship hull surface. Moreover, the Neumann-Kelvin method can be used to solve wave and current coupling problems(e.g., Xie *et al.* (2015), Liu and Falzarano (2016), Guha and Falzarano (2016)). As the result of this paper, although the Neumann-Kelvin method is limited, it may still be valuable in practical use for cautious considerations.

research.

References

Michell, J. (1898), "The wave-resistance of a ship", *Phil. Mag.*, **45**(5), 106-123.

Havelock, T. (1928), "Wave resistance", *Proceedings of the Royal Society of London. Series A, Containing Papers of a Mathematical and Physical Character*, **118**(779), 24-33.

Havelock, T. (1932), "The theory of wave resistance", *Proceedings of the Royal Society of London. Series A, Containing Papers of a Mathematical and Physical Character*, **138**(835), 339-348.

Peters, A.S. (1949), "A new treatment of the ship wave problem", *Communications on pure and applied mathematics*, **2**(2-3), 123-148.

Noblesse, F. (1981), "Alternative integral representations for the Green function of the theory of ship wave resistance", *J. Eng. Math.*, **15**(4), 241-265.

Hess, J.L. and Smith, A. (1962), "Calculation of non-lifting potential flow about arbitrary three-dimensional bodies", Technical Report, DTIC Document.

Hess, J. and Smith, A. (1967), "Calculation of potential flow about arbitrary bodies", *Progr. Aerosp. Sci.*, **8**, 1-138.

Newman, J. (1987), "Evaluation of the wave-resistance green function. I: The double integral", *J. Ship Res.*, **31**(2), 79-90.

Ponizy, B. and Noblesse, F. (1994), "Numerical evaluation of free-surface Green functions", *J. Ship Res.*, 193-202.

Baar, J. (1986), "A three-dimensional linear analysis of steady ship motion in deep water", Ph.D. Dissertation, Brunel University School of Engineering and Design, U.K.

Baar, J. and Price, W. (1988), "Developments in the Calculation of the Wavemaking Resistance of Ships", in "Proceedings of the Royal Society of London A: Mathematical, Physical and Engineering Sciences", The Royal Society, **416**, 115-147.

Bessho, M. (1964), "On the fundamental function in the theory of the wave-making resistance of ships", *Mem. Def. Academ., Jap.*, **4**(2), 99-119.

Ursell, F. (1960), "On Kelvin's ship-wave pattern", *J. Flu. Mech.*, **8**(03), 418-431.

Marr, G.P. (1996), "An investigation of Neumann-Kelvin ship wave theory and its application to yacht design", Ph.D. Dissertation, ResearchSpace Auckland, U.S.A.

Wang, H. and Rogers, J. (1989), "Numerical evaluation of the complete wave-resistance Green's function using Bessho's approach", *Proceedings of the 5th International Conference on Numerical Ship Hydrodynamics*.

Abramowitz, M. and Stegun, I.A. (1964), *Handbook of Mathematical Functions: with Formulas, Graphs, and Mathematical Tables*, Courier Corporation, Washington D.C., U.S.A.

Levin, D. (1982), "Procedures for computing one-and two-dimensional integrals of functions with rapid irregular oscillations", *Math. Comput.*, **38**(158), 531-538.

Levin, D. (1997), "Analysis of a collocation method for integrating rapidly oscillatory functions", *J. Comput. Appl. Math.*, **78**(1), 131-138.

Faddeyeva, V., Terentev, N. and Fok, V. (1961), *Tables of the probability integral for complex argument*, Pergamon Press, Oxford, U.K.

Motygin, O.V. (2014), *On Computation of Oscillating Integrals of Ship-Wave Theory*, arXiv Preprint arXiv:1411.0321.

Maruo, H. (1966), "A note on the higher order theory of thin ships", *Bulletin of the Faculty of Engineering,*

Yokohama National University, **15**, 1-21.

Eggers, K.W.H. (1966), "On second order contribution to ship waves and wave resistance", *Proceedings of the 6th Symposium on Naval Hydrodynamics*, Washington, U.S.A.

Wehausen, J.V. (1967), *Use of Lagrangian Coordinates for Ship Wave Resistance (First and Second Order Thin-Ship Theory)*, Technical Report, DTIC Document.

Yim, B. (1968), "Higher order wave theory of ships", *J. Ship Res.*, 237-245.

Guilloton, R. (1964), "L'etude theorique du bateau en fluide parfait", *Bull. Assoc. Tech. Maritime Aero.*, **64**, 537-552.

Guilloton, R. (1965), "La pratique du calcul des isobares sur une carène linéarisée", *Bull. Ass. Tech. Mar. Aeronaut.*, **65**, 379-394.

Dawson, C. (1977), "A practical computer method for solving ship-wave problems", *Proceedings of the 2nd International Conference on Numerical Ship Hydrodynamics*, DTIC Document, 30-38.

Han, P. and Olson, M. (1987a), "An adaptive boundary element method", *J. Numer. Meth. Eng.*, **24**(6), 1187-1202.

Schultz, W.W. and Hong, S. (1989a), "Solution of potential problems using an overdetermined complex boundary integral method", *J. Comput. Phys.*, **84**(2), 414-440.

Cao, Y. (1991a), *Computation of Nonlinear Gravity Waves by a Desingularized Boundary Integral Method*, Technical Report, DTIC Document.

Raven, H.C. (1998), "Wave pattern analysis applied to nonlinear ship wave calculations", *Proceedings of the 13th International Workshop on Water Waves and Floating Bodies*, the Netherlands.

Raven, H. (1996), "A solution method for the nonlinear ship wave resistance problem", Ph.D. Dissertation, Scheepsbouwkundig Ingenieur Geboren Te Utrecht, Amsterdam, the Netherlands.

Janson, C.E. (1997), *Potential flow panel methods for the calculation of free-surface flows with lift*, Chalmers University of Technology, Sweden.

Hess, J.L. *et al.* (1980), "A higher order panel method for three-dimensional potential flow", *Proceedings of the 7th Australasian Conference on Hydraulics and Fluid Mechanics*, Institution of Engineers, Australia, 517.

Guha, A. (2012), "Development of a computer program for three dimensional frequency domain analysis of zero speed first order wave body interaction", Ph.D. Dissertaion, Texas A&M University, College Station, U.S.A.

Guha, A. and Falzarano, J. (2015a), "Application of multi objective genetic algorithm in ship hull optimization", *Ocean Syst. Eng.*, **5**(2), 91-107.

Guha, A. and Falzarano, J. (2015b), "The effect of hull emergence angle on the near field formulation of added resistance", *Ocean Eng.*, **105**, 10-24.

Brard, R. (1972), "The representation of a given ship form by singularity distributions when the boundary condition on the free surface is linearized", *J. Ship Res.*, **16**(1).

Wehausen, J.V. and Laitone, E.V. (1960), "Surface waves", in "Fluid Dynamics/Strömungsmechanik", Springer, 446-778.

Gentleman, W.M. (1972), "Implementing Clenshaw-Curtis quadrature, I methodology and experience", *Commun. ACM*, **15**(5), 337-342.

Han, P. and Olson, M. (1987b), "An adaptive boundary element method", *J. Numer. Meth. Eng.*, **24**(6), 1187-1202.

Schultz, W.W. and Hong, S. (1989b), "Solution of potential problems using an overdetermined complex bound-

ary integral method", *J. Comput. Phys.*, **84**(2), 414-440.

Musker, A. (1989), "A panel method for predicting ship wave resistance", *Proceedings of the 17th Symposium on naval hydrodynamics*, 143-150.

Cao, Y. (1991b), *Computation of Nonlinear Gravity Waves by a Desingularized Boundary Integral Method*, Technical Report, DTIC Document.

Todd, F.H. (1963), *Series 60 Methodical Experiments with Models of Single-Screw Merchant Ships*, Technical Report, David Taylor Model Basin Washington, U.S.A.

Lewis, E.V. (1988), *Principles of Naval Architecture Second Revision*, Jersey: SNAME.

Yu, M. and Falzarano, J. (2017), "Comparison of direct pressure integration and wave cut analysis for wave resistance calculations using nonlinear Rankine panel method", *J. Ocean Eng. Mar. Energy*.

Xie, Z.T., Yang, J.M., Hu, Z.Q., Zhao, W.H. and Zhao, J.R. (2015), "The horizontal stability of an FLNG with different turret locations", *J. Nav. Archit. Ocean Eng.*, **7**(2), 244-258.

Liu, Y. and Falzarano, J.M. (2016), "Suppression of irregular frequency in multi-body problem and free-surface singularity treatment", in "*Proceedings of the 35th International Conference on Ocean, Offshore and Arctic Engineering*", *American Society of Mechanical Engineers*.

*Guha, A. and Falzarano, J. (2016), "Estimation of hydrodynamic forces and motion of ships with steady forward speed", Int. Shipbuild. Progr., **62**(3-4), 113-138.*

MK